Bioinformatic and MD analysis of N501Y SARS-CoV-2 (UK) variant*

Marko Jukić[1,2][0000−0001−6083−5024]✉, Sebastjan Kralj[1][0000−0000−0000−0000], Natalia Nikitina[3][0000−0002−0538−2939], and Urban Bren[1,2][0000−0000−0000−0000]✉

[1] University of Maribor, Faculty of Chemistry and Chemical Engineering, Laboratory of Physical Chemistry and Chemical Thermodynamics, Smetanova ulica 17, SI-2000 Maribor, Slovenia, {marko.jukic,urban.bren}@um.si

[2] University of Primorska, Faculty of Mathematics, Natural Sciences and Information Technologies, Glagoljaška 8, SI-6000 Koper, Slovenia

[3] Institute of Applied Mathematical Research, Karelian Research Center of the Russian Academy of Sciences, Pushkinskaya 11, 185910, Petrozavodsk, Russia

Abstract. COVID-19 is a disease caused by severe acute respiratory syndrome coronavirus 2 or SARS-CoV-2 pathogen. Although a number of new vaccines are available to combat this threat, a high prevalence of novel mutant viral variants is observed in all world regions affected by this infection. Among viral proteomes, the highly glycosylated spike protein (Sprot) of SARS-CoV-2 has received the most attention due to its interaction with the host receptor ACE2. To understand the mechanisms of viral variant infectivity and the interaction of the RBD of Sprot with the host ACE2, we performed a large-scale mutagenesis study of the RBD-ACE2 interface by performing 1780 point mutations *in silico* and identifying the ambiguous stabilisation of the interface by the most common point mutations described in the literature. Furthermore, we pinpointed the N501Y mutation at the RBD of Sprot as profoundly affecting complex formation and confirmed greater stability of the N501Y mutant compared to wild-type (WT) viral S protein by molecular dynamics experiments. These findings could be important for the study and design of upcoming vaccines, PPI inhibitor molecules, and therapeutic antibodies or antibody mimics.

Keywords: COVID-19 · SARS-CoV-2 · point mutation · SARS-CoV-2 variants · protein-protein interactions · drug design.

1 Introduction

In 1962, scientists isolated a new group of viruses that cause cold (enveloped positive-sense single-stranded (+ssRNA) RNA virus). They named this new

* Supported by the Slovenian Ministry of Science and Education infrastructure project grant HPC-RIVR, by the Slovenian Research Agency (ARRS) programme and project grants P2-0046 and J1-2471, and by Slovenian Ministry of Education, Science and Sports programme grant OP20.04342.

group of viruses, *coronaviruses* after their characteristic morphological appearance, namely they are named after crown spikes located on their surface [9].

The viruses from the *Coronaviridae* family have rarely attracted attention over the last half-century. The first example was in 2003, when the coronavirus caused an outbreak of SARS (Severe Acute Respiratory Syndrome; pathogen virus named SARS-CoV) in mainland China and Hong Kong. Another example was in 2012 when the Middle East coronavirus of the respiratory syndrome (MERS-CoV) led to an outbreak of the Middle East respiratory syndrome (MERS) in Saudi Arabia mainland China and the United Arab Emirates and the Republic of Korea [16, 12, 26].

In late 2019, SARS-CoV-2, a member of the *Coronaviridae* family, appeared in Wuhan, China, and a creeping spread among the human population has begun [39]. The WHO declared a pandemic on 11 March 2020 [25, 14]. At the time of writing this article, the COVID-19 disease (caused by SARS-CoV-2) has spread rapidly worldwide, claiming more than **3** million lives (*https://www.worldometers.info/coronavirus/coronavirus-death-toll/*). As the SARS-CoV-2 virus has become a critical health problem, scientists immediately began research to clarify the virus' mode of action [36]. COVID-19 disease is of grave global concern because, while the majority of cases displays mild symptoms, a variable percentage (0.2 to > 5 %!) of patients progresses to pneumonia and multi-organ failure leading to potential death, especially without medical assistance [13, 31, 27].

As of now, we have registered vaccines against SARS-CoV-2 [1, 7]. but still no antivirals and only a few of therapeutic options for COVID-19 treatment [28, 23]. As vaccines represent the flagship in the fight against COVID-19 pandemic, high viral mutation rate can translate to changes in the structures of key viral proteins rendering available vaccines ineffective [30].

In late 2020, new SARS-CoV-2 variants was reported; mainly B.1.1.7 variant (UK variant, named alpha by WHO as of 7th June, 2021; https://www.who.int/) and B.1.351 variant (beta) or South African variant [35, 33]. Both variants carry N501Y mutation in the RBD (receptor binding domain) of the Sprot (spike protein) that is associated with increased viral transmission [11]. The South African variant carries K417N and E484K mutations in the Sprot that are potentially responsible for the diminished binding of viral Sprot to host antibodies [38]. In Brazil, P.1 (gamma) variant with known N501Y, E484K and novel K417T mutation was reported [10].

In early 2021, a novel SARS-CoV-2 variant B.1.617 (delta) nicknamed "the double mutant" or Indian variant was reported causing infections in India and slowly spreading all over the world via global travel practices [8, 40, 29, 6]. Acquired key mutations in S protein, especially at the receptor binding domain (RBD) are under investigation (delta plus) due to potential of greater infectivity, transmissibility, or even the potential to escape host immune responses [34]. Summary of main SARS-CoV-2 variants is provided in Table 1. To this end, we sought to investigate a staple **N501Y** mutation on RBD binding domain present in B.1.1.7, B.1.351 and P.1 variants via FoldX mutational scan, molecular dynamic (MD) analysis and compare it to wild type.

Table 1. Summary of SARS-CoV-2 variants

Variant[1]	*Alternative name*	*Sprot/ all mutations*	*Key mutations*	*Comment*
B.1.1.7	UK Variant-alpha	8/23	E69/70 del 144Y del **N501Y** (RBD) A570D P681H	higher transmissibility
B.1.351	South African Variant-beta	9/21	K417N (RBD) E484K (RBD) **N501Y** (RBD) orf1b del	escape host immune response
P.1	Brasil Variant-gamma	10/17	K417N/T (RBD) E484K (RBD) **N501Y** (RBD) orf1b del	under research
B.1.617	Indian Variant-delta	7/23	G142D delta156-157/R158G. A222V **L452R** (RBD) **T478K** (RBD) D614G P681R D950N	under research

[1]Other known variants are COH.20G, S Q677H (Midwest variant) and L452R, B1429; reference https://www.uniprot.org/uniprot/P0DTC

2 Methods and Results

2.1 FoldX calculations – mutagenesis study

FoldX relative free energies ($\Delta\Delta G$) for Spro RBD mutants were calculated using FoldX, version 5 [5]. To analyse the influence of the FoldX point mutations along with FoldX optimisation, 3D structures of wild type along with FoldX mutants were iteratively used for $\Delta\Delta G$ prediction. Point mutations were performed using the `--command=BuildModel` switch and supplied individual_list.txt file with `--mutant-file` switch. Number of runs was set at default value of 5. All other options were set to default, including temperature (298 K), ionic strength (0.05 M), and pH (7), VdWDesign 2 strong, clashCapDesign 5, backBoneAtoms false, dipoles true and complexClashes parameter set to 1. *Inhouse* script was prepared to calculate all possible mutations of RBD binding domain of SARS-CoV-2 S protein (PDB ID: 6M0J) with sequence from K417 towards Y505 (length of 89) for a total of 1780 point mutations (Table 2).

In the mutagenesis study, individual point mutation calculations were repeated once and mutations with no structural change left for validation purposes where all no-change mutation produced $\Delta\Delta G$ energies below 0.1 kcal/mol.

Table 2. Sequences used for mutagenesis study

Spike protein length	229
>6M0J_2—Chain E—Spike protein S1—Severe acute respiratory syndrome coronavirus 2 (2697049) RVQPTESIVRFPNITNLCPFGEVFNATRFASVYAWNRKRISNCVADYSVLYN SASFSTFKCYGVSPTKLNDLCFTNVYADSFVIRGDEVRQIAPGQTG**KIADY** **NYKLPDDFTGCVIAWNSNNLDSKVGGNYNYLYRLFRKSNLKPFE** **RDISTEIYQAGSTPCNGVEGFNCYFPLQSYGFQPTNGVGY**QPYRV VVLSFELLHAPATVCGPKKSTNLVKNKCVNFHHHHH	
Mutagenesis study sequence (RBD) length	89
KIADYNYKLPDDFTGCVIAWNSNNLDSKVGGNYNYLYRLFRKSNLKPFERD ISTEIYQAGSTPCNGVEGFNCYFPLQSYGFQPTNGVGY	

2.2 Model preparation

The 2.45 Å crystal structure (PDB ID: 6M0J) of SARS-CoV-2 spike receptor-binding domain bound with ACE2 was obtained via RCSB PDB Database [21]. Chain E (Spike protein S1) was chosen for further work where analysis of protein-protein interaction (PPI) with chain A (Angiotensin-converting enzyme 2) was conducted. Complex was prepared Yasara STRUCTURE (19.6.6.L.64) software [20]. Missing hydrogens were added, missing bonds and bond orders set, overlapping atoms adjusted, rebuild side-chains with missing atoms, hydrogen bonds optimized, proteins capped (Ace, Nma) and residue ionisation assigned at $pH = 7.4$ [19, 18].

The interface of Sprot RBD domain in up(open) conformation was referenced against SARS-CoV-2 S trimer, S-open complex (PDB ID: 7DK3) where superimposition of chain E from 6M0J and chain C from 7DK3 with an all atom RMSD of 1.429 Å produced a nearly similar conformation of S protein RBD. Carbohydrates were not considered in the vicinity of RBD interface (Figure 1).

2.3 Molecular Dynamics

We performed MD simulations of the chimeric receptor-binding domain (RBD) of the SARS-CoV-2 spike protein bound to the human Angiotensin-converting enzyme 2 (ACE2) to study the effect of mutational changes to binding dynamics of the protein complex. The simulation inputs were prepared using the CHARMM-GUI web interface for the CHARMM biomolecular simulations program [4, 15]. The input structure PDB ID: 6VW1 was chosen among the many RBD-ACE2 structures due to its superior resolution and high scoring percentile ranks provided by the web interface of PDB [32].

Using the CHARMM-GUI server, we generated an additional mutant N501 using the built-in functionality. The mutation was chosen due to the ever-increasing prevalence which may indicate that this mutation, occurring in the RBD binding site increases affinity for the host ACE2 [3]. Glycans present in the structure were removed beforehand since they were not present in the interaction site

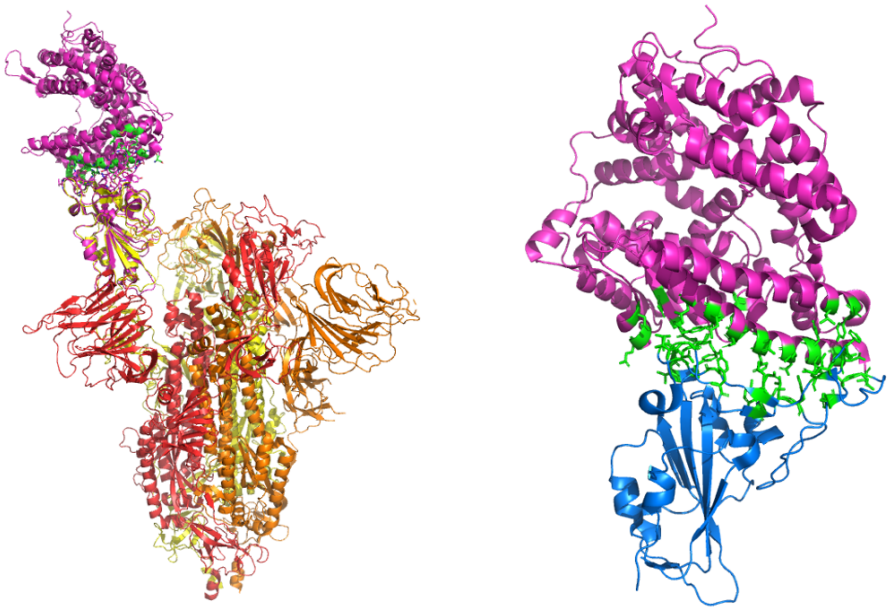

Fig. 1. Left: 7dk3 with S protein chains A B and C colored red, orange and yellow respectively and superimposed 6m0j colored magenta. Right: 6m0j complex where chain A (ACE2) is colored magenta, chain E (RBD) colored blue and PPI interface emphasized in green color. All models are depicted with ribbon presentation.

and would increase computing time. Both protein structures were solvated using TIP3P water and neutralized using Na^+ and Cl^- ions (0.1M) to approximate physiological conditions. To remove existing atomic clashes and optimization of the atomic geometry, 50 steps of the steepest descent and 500 steps of adopted basis Newton-Raphson energy minimization was performed. The final step of equilibration was a 1ns NVT molecular dynamics simulation during which the protein was heated to 310.15 K using the hoover heat bath with the integration time-step set to 1 fs.

Final molecular dynamics production runs were carried out using NPT ensemble with periodic boundary conditions applied, the time-step set to 2 fs and the thermostat set to 310.15 K. Non-bonded interaction cutoff was achieved using a force-based switching function between 12 and 16 Å. Bonds to hydrogens were constrained using the SHAKE algorithm. The CHARMM36m force field was used for all simulations.

For both RBD-ACE2 structures the production runs were generated using GPU acceleration with the final analysis performed on the last 180 ns of the production run, with the first 20 ns of the production runs ignored in order to minimize the error arising from different initial velocity seeds.

3 Discussion

Structural inspection and superimposition of complexes of Sprot-ACE2 (PDB ID: 6M0J) and Sprot open conformation (PDB ID: 7DK3) the Sprot RBD-ACE2 PPI interface was identified and key RBD residues in contact with ACE2 defined as following: 417 LYS, 445 VAL, 446 GLY, 449 TYR, 453 TYR, 455 LEU, 456 PHE, 473 TYR, 475 ALA, 476 GLY, 484 GLU, 486 PHE, 487 ASN, 489 TYR, 493 GLN, 496 GLY, 498 GLN, 500 THR, 501 ASN, 502 GLY, 503 VAL, 505 TYR. Literature reported key mutations on this interface such as E484K - S African variant that could escape immune responses, Q493N or Q493Y with reduced host ACE2-binding affinity in vitro, N501Y UK and S African variant that influences virulence or N501T with reduced host ACE2-binding affinity in vitro all according to P0DTC2 Uniprot reference.

Lately, two key mutations L452R and E484Q from Indian variant are under investigation [8]. We conducted a full RBD 417-505 mutagenesis study using FoldX in order to asses these key mutations and their effect on the stability of the system, in total 1780 point mutations (Figure 2) [42].

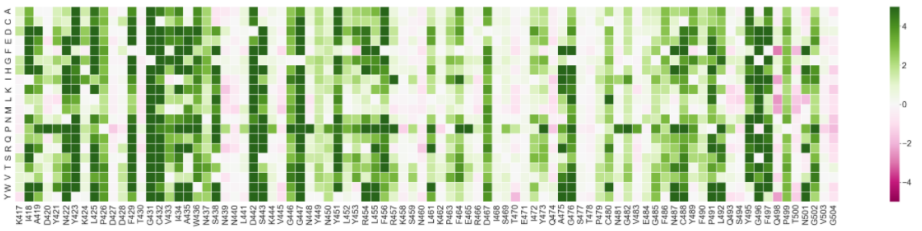

Fig. 2. Complete RBD-ACE2 interface mutagenesis heatmap where deep green color indicates positive FoldX force field Δ energies (destabilising) and deep purple contrasting positive FoldX force field Δ energies (stabilising).

We observed FoldX total energies of 0.374201, 0.622215 and -0.950612 kcal/mol upon point mutations E484K, Q493N and Q493Y respectively. All mutations are postulated as non-significantly influencing the stability of RBD-ACE2 complex. Literature reports on reduced binding affinity towards ACE2 but our preliminary results indicate the complex formation is more complex than initially postulated [17]. Indeed, the literature corroborates our observations [37].

Furthermore, L452R and E484Q point mutations from Indian viral variant display insignificant FoldX force field Δ energies of 0.0424621, 0.0912967 kcal/mol, respectively [2, 24, 41]. On the contrary, FoldX force field Δ energies of 6.18517 and -0.449581 kcal/mol were observed for UK variant point mutations N501Y and N501T, respectively, indicating a predictable effect of N501Y point mutation of RBD-ACE2 binding, an observation confirmed by experimental evaluation [22].

In order to further assess the influence of N501Y point mutation, we conducted a molecular dynamics (MD) experiment on WT RBD-ACE2 and N501Y mutated protein (Figures 3-6).

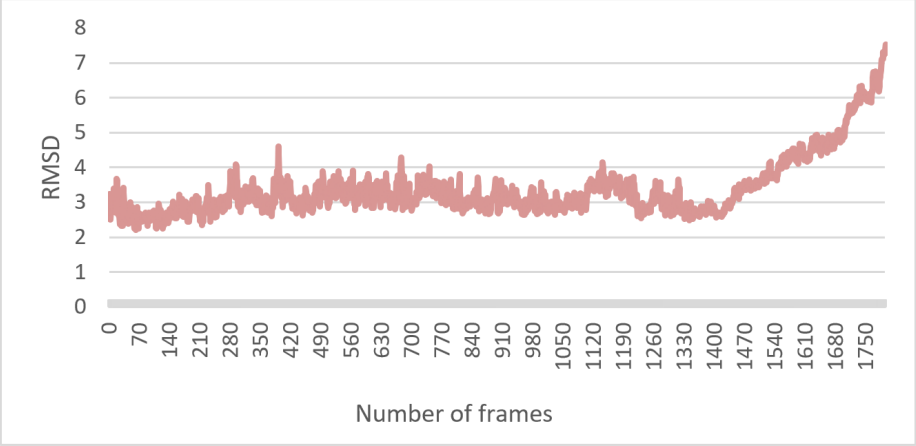

Fig. 3. Root mean square deviation of wild type RBD-ACE2 complex through simulation time

From the 180 ns production runs, it can be observed the point mutated N501Y RBD-ACE2 complex displays comparable conformational stability all along the production run with backbone RMSD of 3.37 ± 0.85Å and radius of gyration $31,69 \pm 0.48$Å versus $2.87 \pm 0,26$Å and radius of gyration of 31.30 ± 0.22Å for WT, respectively. Nevertheless, after the inflection point at 140 ns, the WT experiences a conformational change leading to a linear increase of both measured parameters. The amino acid contact profiles are also distinct as can be observed in Table 3 and 4 where residues with longest contact times at the interface are tabulated.

Wild type RBD after the MD experiment displays a contact surface area of 1126.88Å^2 for RBD interface residues with distance < 5Å away from ACE2, from that 64.37Å^2 falls towards Asp and Glu, $329,84$Å^2 goes to Ser, Thr, Asn and Gln and $597,62$Å^2 towards Ala, Val, Ile, Leu, Met, Phe, Tyr and Trp. Key hydrogen bonds from RBD towards ACE2 are Tyr449-Glu37 (1.88Å), Glu484-Lys31 (1.88Å), Asn487-Tyr83 (2.04Å), Thr500-Gly326 (2.15Å) and Asn501-Gly354 with the distance of 1.98Å. Contrasting the N501Y mutant RBD displays a greater surface of 1348.94Å^2 for residues with distance < 5Å away from ACE2.

Analogously to WT surface analyses 73.35Å^2 falls towards Asp and Glu, 292.17Å^2 goes to Ser, Thr, Asn and Gln and 731.91Å^2 to hydrophobic residues with additional effective contacts via Arg, His, Lys with 130.04Å^2. In the point mutant following key hydrogen bonds are observed: Arg439-Gln325 (1.88Å),

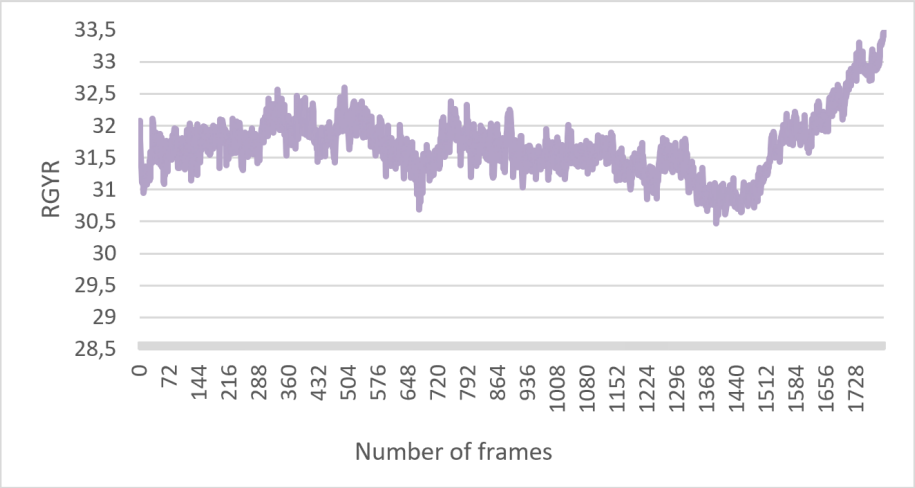

Fig. 4. Radius of Gyration of the wild type RBD-ACE2 complex through simulation time

Asn487-Tyr83 (1.78Å), Thr500-Asp355 (1.87Å) and Gly502-Lys353 with distance of 1.82Å. It is evident the bulky tyrosine at position 501 effectively increases the contact area and optimises the interface interaction profile towards more hydrophobic contacts and conservation of hydrogen bond propensity (Figure 7).

Table 3. Amino-acid residues with the longest time in contact during simulations for N501Y RBD.

RBD residue ID	ACE2 residue ID	Total time in contact (ps)
Tyr501	Lys353	5876
Tyr473	Glu23	455
Ala475	Ser19	272
Ala475	Gln24	361
Asn487	Tyr83	1306
Tyr489	Tyr83	541
Thr500	Asp355	412

4 Conclusions

In 1962, scientists isolated a new group of viruses that cause colds - enveloped positive-sense single-stranded; +ssRNA; RNA viruses. They named this new group of viruses, coronaviruses after their characteristic spikes on their surface. In late 2019/early 2020, a global pandemic was declared by WHO and the new

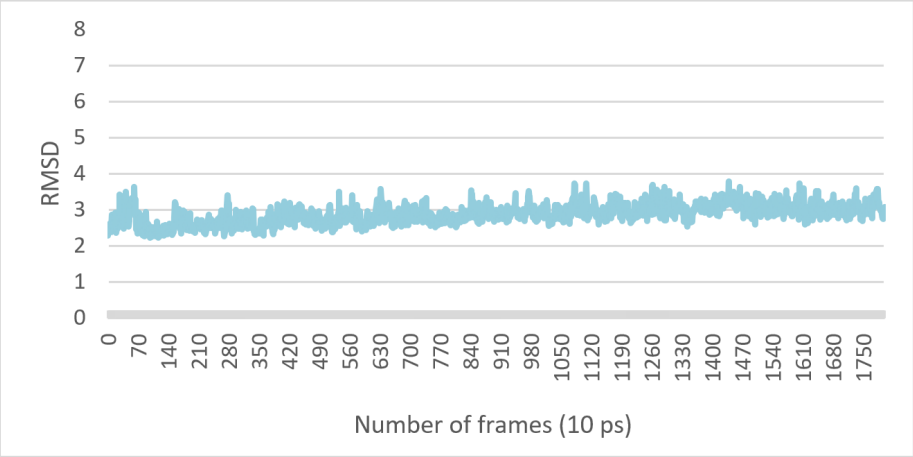

Fig. 5. Root mean square deviation of N501Y mutated RBD-ACE2 complex through simulation time

Table 4. Amino-acid residues with the longest time in contact during simulations for wild type RBD.

RBD residue ID	ACE2 residue ID	Total time in contact (ps)
Thr446	Lys353	550
Tyr449	Asp38	826
Asn487	Tyr83	2285
Tyr489	Tyr83	1100
Ser494	Hsd34	400
Gln498	Tyr41	450
Val503	Gln325	300

pathogen named SARS-CoV-2 from the *Coronaviridae* family was quickly and effectively sequenced and described. Following the introduction of vaccines against the new pathogen, a wide range of viral variants were thoroughly investigated, particularly with regard to vaccine efficacy. To analyze the key profile of the viral Sprot RBD - host ACE2 interaction, we first performed a large-scale mutagenesis study of the RBD-ACE2 interface using FoldX software, where we performed 1780 point mutations *in silico* and identified the ambiguous stabilization of the interface by the most frequent point mutations described in the literature. Indeed, this interface was difficult to quantify under the FoldX force field, but we still identified a profound impact on RBD-ACE2 by the point mutation N501Y. In MD analysis, we confirmed greater stability and enlarged contact area of the N501Y mutant compared to the wild-type (WT) viral S protein. These findings could be of great value for the study and design of upcoming vaccines, PPI inhibitor molecules and therapeutic antibodies or antibody mimics.

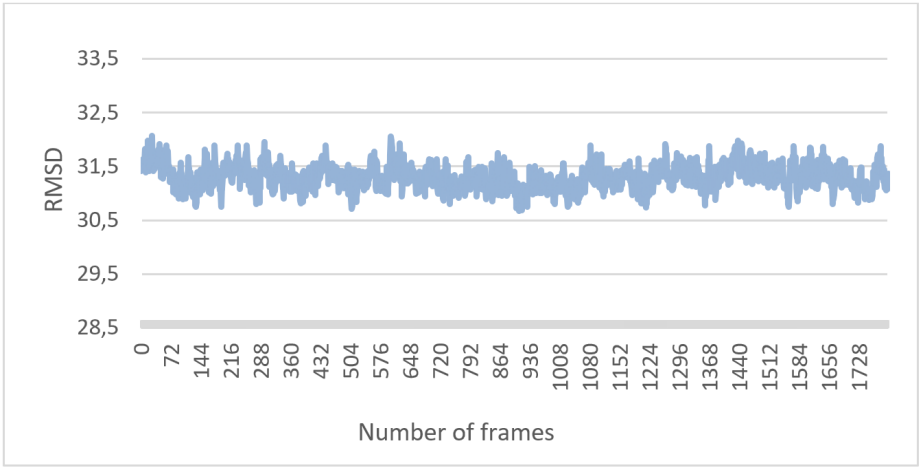

Fig. 6. Radius of gyration of the N501Y mutant RBD-ACE2 complex through simulation time

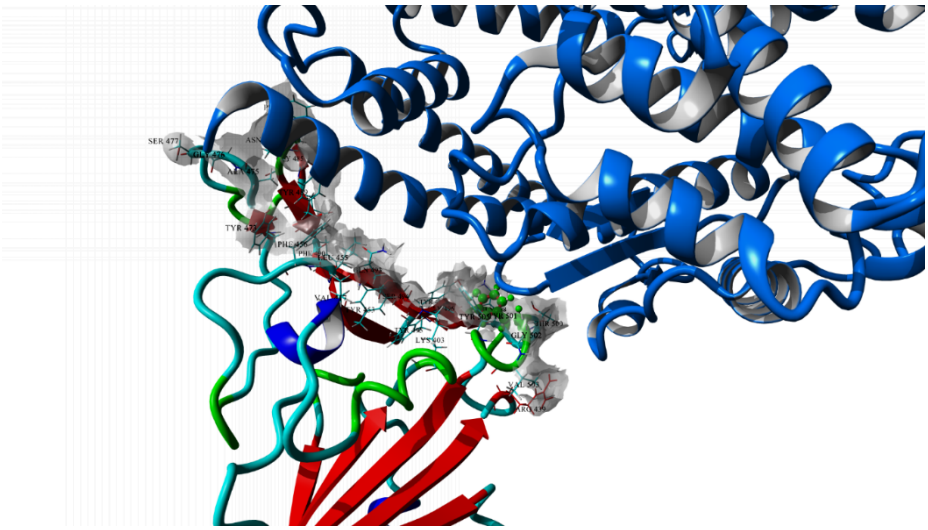

Fig. 7. Sprot RBD-host ACE2 interface for N501Y point mutant. Proteins are depicted in cartoon model representation ACE2 colored blue and RBD in red, green, blue, cyan color with interacting residues in line model, labelled with mutated residue N501Y emphasized as ball and stick model colored green. Surface area of interacting RBD is presented in gray color.

Acknowledgements: We thank Javier Delgado Blanco and Luis Serrano Pubul from FoldX for their support. Heartfelt thanks to Črtomir Podlipnik, a friend and a scientific colleague.

Thank You, participants in the COVID.SI community (www.covid.si and www.sidock.si) for supporting our work. Thank You All!

Conflicts of Interest: The authors declare no conflict of interest.

Abbreviations

ACE2	Angiotensin-converting enzyme 2
MD	Molecular Dynamics
PDB	Protein Data Bank
PPI	Protein-Protein Interactions
RBD	Receptor Binding Domain
WHO	World Health Organisation

References

1. Amanat, F., Krammer, F.: SARS-CoV-2 vaccines: status report. Immunity **52**(4), 583–589 (2020)
2. Banu, S., Jolly, B., Mukherjee, P., Singh, P., Khan, S., Zaveri, L., Shambhavi, S., Gaur, N., Reddy, S., Kaveri, K., et al.: A distinct phylogenetic cluster of Indian severe acute respiratory syndrome coronavirus 2 isolates. Open forum infectious diseases **7**(11), ofaa434 (2020)
3. Bracken, C.J., Lim, S.A., Solomon, P., Rettko, N.J., Nguyen, D.P., Zha, B.S., Schaefer, K., Byrnes, J.R., Zhou, J., Lui, I., et al.: Bi-paratopic and multivalent VH domains block ACE2 binding and neutralize SARS-CoV-2. Nature Chemical Biology **17**(1), 113–121 (2021)
4. Brooks, B.R., Brooks III, C.L., Mackerell Jr, A.D., Nilsson, L., Petrella, R.J., Roux, B., Won, Y., Archontis, G., Bartels, C., Boresch, S., et al.: CHARMM: the biomolecular simulation program. Journal of computational chemistry **30**(10), 1545–1614 (2009)
5. Buß, O., Rudat, J., Ochsenreither, K.: FoldX as protein engineering tool: better than random based approaches? Computational and structural biotechnology journal **16**, 25–33 (2018)
6. Chatterjee, P.: Covid-19: India authorises Sputnik V vaccine as cases soar to more than 180 000 a day (2021)
7. Chen, W.H., Strych, U., Hotez, P.J., Bottazzi, M.E.: The SARS-CoV-2 vaccine pipeline: an overview. Current tropical medicine reports **7**(2), 61–64 (2020)
8. Cherian, S., Potdar, V., Jadhav, S., Yadav, P., Gupta, N., Das, M., Rakshit, P., Singh, S., Abraham, P., Panda, S., et al.: Convergent evolution of SARS-CoV-2 spike mutations, L452R, E484Q and P681R, in the second wave of COVID-19 in Maharashtra, India. BioRxiv (2021)
9. De Wit, E., Van Doremalen, N., Falzarano, D., Munster, V.J.: SARS and MERS: recent insights into emerging coronaviruses. Nature Reviews Microbiology **14**(8), 523–534 (2016)
10. Faria, N.R., Claro, I.M., Candido, D., Franco, L.M., Andrade, P.S., Coletti, T.M., Silva, C.A., Sales, F.C., Manuli, E.R., Aguiar, R.S., et al.: Genomic characterisation of an emergent SARS-CoV-2 lineage in Manaus: preliminary findings. Virological (2021)

11. Gu, H., Chen, Q., Yang, G., He, L., Fan, H., Deng, Y.Q., Wang, Y., Teng, Y., Zhao, Z., Cui, Y., et al.: Adaptation of SARS-CoV-2 in BALB/c mice for testing vaccine efficacy. Science **369**(6511), 1603–1607 (2020)
12. Hilgenfeld, R., Peiris, M.: From SARS to MERS: 10 years of research on highly pathogenic human coronaviruses. Antiviral research **100**(1), 286–295 (2013)
13. Hopkins, J.: Mortality analyses, https://coronavirus.jhu.edu/data/mortality
14. Hui, D.S., Azhar, E.I., Madani, T.A., Ntoumi, F., Kock, R., Dar, O., Ippolito, G., Mchugh, T.D., Memish, Z.A., Drosten, C., et al.: The continuing 2019-nCoV epidemic threat of novel coronaviruses to global health—The latest 2019 novel coronavirus outbreak in Wuhan, China. International journal of infectious diseases **91**, 264–266 (2020)
15. Jo, S., Kim, T., Iyer, V.G., Im, W.: CHARMM-GUI: a web-based graphical user interface for CHARMM. Journal of computational chemistry **29**(11), 1859–1865 (2008)
16. Kahn, J.S., McIntosh, K.: History and recent advances in coronavirus discovery. The Pediatric infectious disease journal **24**(11), S223–S227 (2005)
17. Khan, A., Zia, T., Suleman, M., Khan, T., Ali, S.S., Abbasi, A.A., Mohammad, A., Wei, D.Q.: Higher infectivity of the SARS-CoV-2 new variants is associated with K417N/T, E484K, and N501Y mutants: An insight from structural data. Journal of cellular physiology (2021)
18. Krieger, E., Dunbrack, R.L., Hooft, R.W., Krieger, B.: Assignment of protonation states in proteins and ligands: Combining pK a prediction with hydrogen bonding network optimization. In: Computational Drug Discovery and Design, pp. 405–421. Springer (2012)
19. Krieger, E., Nielsen, J.E., Spronk, C.A., Vriend, G.: Fast empirical pKa prediction by Ewald summation. Journal of molecular graphics and modelling **25**(4), 481–486 (2006)
20. Krieger, E., Vriend, G.: New ways to boost molecular dynamics simulations. Journal of computational chemistry **36**(13), 996–1007 (2015)
21. Lan, J., Ge, J., Yu, J., Shan, S., Zhou, H., Fan, S., Zhang, Q., Shi, X., Wang, Q., Zhang, L., et al.: Structure of the SARS-CoV-2 spike receptor-binding domain bound to the ACE2 receptor. Nature **581**(7807), 215–220 (2020)
22. Leung, K., Shum, M.H., Leung, G.M., Lam, T.T., Wu, J.T.: Early transmissibility assessment of the N501Y mutant strains of SARS-CoV-2 in the United Kingdom, October to November 2020. Eurosurveillance **26**(1), 2002106 (2021)
23. Li, H., Zhou, Y., Zhang, M., Wang, H., Zhao, Q., Liu, J.: Updated approaches against SARS-CoV-2. Antimicrobial agents and chemotherapy **64**(6), e00483–20 (2020)
24. Li, Q., Wu, J., Nie, J., Zhang, L., Hao, H., Liu, S., Zhao, C., Zhang, Q., Liu, H., Nie, L., et al.: The impact of mutations in SARS-CoV-2 spike on viral infectivity and antigenicity. Cell **182**(5), 1284–1294 (2020)
25. Li, Q., Guan, X., Wu, P., Wang, X., Zhou, L., Tong, Y., Ren, R., Leung, K.S., Lau, E.H., Wong, J.Y., et al.: Early transmission dynamics in Wuhan, China, of novel coronavirus–infected pneumonia. New England journal of medicine (2020)
26. Lu, G., Wang, Q., Gao, G.F.: Bat-to-human: spike features determining 'host jump'of coronaviruses SARS-CoV, MERS-CoV, and beyond. Trends in microbiology **23**(8), 468–478 (2015)
27. Lu, R., Zhao, X., Li, J., Niu, P., Yang, B., Wu, H., Wang, W., Song, H., Huang, B., Zhu, N., et al.: Genomic characterisation and epidemiology of 2019 novel coronavirus: implications for virus origins and receptor binding. The lancet **395**(10224), 565–574 (2020)

28. McKee, D.L., Sternberg, A., Stange, U., Laufer, S., Naujokat, C.: Candidate drugs against SARS-CoV-2 and COVID-19. Pharmacological research **157**, 104859 (2020)
29. Moelling, K.: Within-host and between-host evolution in SARS-CoV-2—new variant's source. Viruses **13**(5), 751 (2021)
30. Naqvi, A.A.T., Fatima, K., Mohammad, T., Fatima, U., Singh, I.K., Singh, A., Atif, S.M., Hariprasad, G., Hasan, G.M., Hassan, M.I.: Insights into SARS-CoV-2 genome, structure, evolution, pathogenesis and therapies: Structural genomics approach. Biochimica et Biophysica Acta (BBA)-Molecular Basis of Disease **1866**(10), 165878 (2020)
31. O'Driscoll, M., Dos Santos, G.R., Wang, L., Cummings, D.A., Azman, A.S., Paireau, J., Fontanet, A., Cauchemez, S., Salje, H.: Age-specific mortality and immunity patterns of SARS-CoV-2. Nature **590**(7844), 140–145 (2021)
32. Shang, J., Ye, G., Shi, K., Wan, Y., Luo, C., Aihara, H., Geng, Q., Auerbach, A., Li, F.: Structural basis of receptor recognition by SARS-CoV-2. Nature **581**(7807), 221–224 (2020)
33. Tegally, H., Wilkinson, E., Giovanetti, M., Iranzadeh, A., Fonseca, V., Giandhari, J., Doolabh, D., Pillay, S., San, E.J., Msomi, N., et al.: Emergence and rapid spread of a new severe acute respiratory syndrome-related coronavirus 2 (SARS-CoV-2) lineage with multiple spike mutations in South Africa. MedRxiv (2020)
34. Teng, S., Sobitan, A., Rhoades, R., Liu, D., Tang, Q.: Systemic effects of missense mutations on SARS-CoV-2 spike glycoprotein stability and receptor-binding affinity. Briefings in bioinformatics **22**(2), 1239–1253 (2021)
35. Volz, E., Mishra, S., Chand, M., Barrett, J.C., Johnson, R., Geidelberg, L., Hinsley, W.R., Laydon, D.J., Dabrera, G., O'Toole, Á., et al.: Transmission of SARS-CoV-2 Lineage B. 1.1. 7 in England: Insights from linking epidemiological and genetic data. MedRxiv pp. 2020–12 (2021)
36. Wang, C., Horby, P.W., Hayden, F.G., Gao, G.F.: A novel coronavirus outbreak of global health concern. The lancet **395**(10223), 470–473 (2020)
37. Wang, W.B., Liang, Y., Jin, Y.Q., Zhang, J., Su, J.G., Li, Q.M.: E484K mutation in SARS-CoV-2 RBD enhances binding affinity with hACE2 but reduces interactions with neutralizing antibodies and nanobodies: Binding free energy calculation studies. bioRxiv (2021)
38. Wibmer, C.K., Ayres, F., Hermanus, T., Madzivhandila, M., Kgagudi, P., Oosthuysen, B., Lambson, B.E., De Oliveira, T., Vermeulen, M., Van der Berg, K., et al.: SARS-CoV-2 501Y. V2 escapes neutralization by South African COVID-19 donor plasma. Nature medicine **27**(4), 622–625 (2021)
39. Wu, F., Zhao, S., Yu, B., Chen, Y.M., Wang, W., Song, Z.G., Hu, Y., Tao, Z.W., Tian, J.H., Pei, Y.Y., et al.: A new coronavirus associated with human respiratory disease in china. Nature **579**(7798), 265–269 (2020)
40. Yadav, P., Sapkal, G.N., Abraham, P., Ella, R., Deshpande, G., Patil, D.Y., Nyayanit, D., Gupta, N., Sahay, R.R., Shete, A.M., et al.: Neutralization of variant under investigation B. 1.617 with sera of BBV152 vaccinees. bioRxiv (2021)
41. Yadav, P.D., Mohandas, S., Shete, A.M., Nyayanit, D.A., Gupta, N., Patil, D.Y., Sapkal, G.N., Potdar, V., Kadam, M., Kumar, S., et al.: SARS CoV-2 variant B. 1.617. 1 is highly pathogenic in hamsters than B. 1 variant. bioRxiv (2021)
42. Zhang, Y., Wang, L., Ardejani, M.S., Aris, N.F., Li, X., Orner, B.P., Wang, F.: Mutagenesis study to disrupt electrostatic interactions on the twofold symmetry interface of Escherichia coli bacterioferritin. The Journal of Biochemistry **158**(6), 505–512 (2015)